AD-A070 462 NAVAL RESEARCH LAB WASHINGTON DC F/G 20/9
LONG-PULSE LASER-PLASMA INTERACTIONS AT 10 TO THE 12TH POWER -1--ETC(U)
JUN 79 B H RIPIN, R R WHITLOCK, F C YOUNG

UNCLASSIFIED NRL-MR-3965 NL

| OF |
AD
A070462

END
DATE
FILMED
7-79
DDC

LEVEL II (12) 85

NRL Memorandum Report 3965

Long-Pulse Laser-Plasma Interactions At 10^{12}-10^{15} W/cm^2

B. H. Ripin, R. R. Whitlock, F. C. Young,
S. P. Obenschain, E. A. McLean and R. Decoste

Plasma Physics Division

June 15, 1979

NAVAL RESEARCH LABORATORY
Washington, D.C.

SECURITY CLASSIFICATION OF THIS PAGE (When Data Entered)

REPORT DOCUMENTATION PAGE

READ INSTRUCTIONS BEFORE COMPLETING FORM

1. REPORT NUMBER: NRL Memorandum Report 3965
2. GOVT ACCESSION NO.:
3. RECIPIENT'S CATALOG NUMBER:

4. TITLE (and Subtitle): LONG-PULSE LASER-PLASMA INTERACTIONS AT 10^{12}-10^{15} W/cm² sq. cm. (10 to the 12th power - 10 to the 15th power)

5. TYPE OF REPORT & PERIOD COVERED: Interim report on a continuing NRL problem

6. PERFORMING ORG. REPORT NUMBER:

7. AUTHOR(s): B. H. Ripin, R. R. Whitlock, F. C. Young, S. P. Obenschain, E. A. McLean and R. Decoste

8. CONTRACT OR GRANT NUMBER(s):

9. PERFORMING ORGANIZATION NAME AND ADDRESS: Naval Research Laboratory, Washington, D. C. 20375

10. PROGRAM ELEMENT, PROJECT, TASK AREA & WORK UNIT NUMBERS: 67H02-29A

11. CONTROLLING OFFICE NAME AND ADDRESS: Department of Energy, Washington, D. C. 20545

12. REPORT DATE: June 15, 1979

13. NUMBER OF PAGES: 11

14. MONITORING AGENCY NAME & ADDRESS (if different from Controlling Office)

15. SECURITY CLASS. (of this report): Unclassified

15a. DECLASSIFICATION/DOWNGRADING SCHEDULE

(11) 15 Jun 79 (12) 42 p.

16. DISTRIBUTION STATEMENT (of this Report)

Approved for public release; distribution unlimited.

17. DISTRIBUTION STATEMENT (of the abstract entered in Block 20, if different from Report)

(14) NRL-MR-3965

18. SUPPLEMENTARY NOTES

Work performed at the Naval Research Laboratory under auspices of the Department of Energy.

19. KEY WORDS (Continue on reverse side if necessary and identify by block number)

Laser fusion
Plasma
Ablation
Absorption
Heat transport

10 to the 12th and 10 to the 15th power W/sq.cm

20. ABSTRACT (Continue on reverse side if necessary and identify by block number)

Laser-plasma interaction physics including absorption, plasma formation, heating, plasma expansion and energy transport, are examined for 3-nsec Nd-laser irradiances between 10^{12} W/cm² and 10^{15} W/cm². Efficient energy deposition and conditions favorable to ablative acceleration are found at 10^{12}-10^{13} W/cm² whereas reduced absorption, hot electrons and fast ions are seen at 7 $\times 10^{14}$ W/cm². Suitability of the observed physics to laser-pellet fusion is discussed.

7 times 10 to the 14th power W/sq cm.

10 to the 12th to 10 to the 13th power W/sq. cm.

1 950

DD FORM 1 JAN 73 1473 EDITION OF 1 NOV 65 IS OBSOLETE
S/N 0102-014-6601

SECURITY CLASSIFICATION OF THIS PAGE (When Data Entered)

LONG-PULSE LASER-PLASMA INTERACTIONS AT 10^{12}-10^{15} W/cm^2

Laser fusion experiments with long-pulse, low-irradiance 1.06 μm laser pulses have been initiated to study the interaction physics and ablative acceleration of thin foil targets under conditions which avoid the undesirable physics of short-pulse high-irradiance (<1 nsec, >10^{15} W/cm^2) interactions.[2,3] These unwanted effects at high irradiance include: reduced light absorption due to the Brillouin backscatter instability, energetic electrons (tens-of-keV), high energy ions that do not couple momentum efficiently to an imploding pellet, and inhibited thermal conductivity which reduce hydrodymanic efficiency and increase the symmetry requirements of the irradiation for laser-pellet fusion.

In contrast, Nd-laser-plasma experiments reported here at low irradiance (10^{12} - 10^{13} W/cm^2) with 3-nsec pulses show: efficient light absorption (80-90%) with negligible Brillouin backscatter, electron distributions with little or no energetic tails near classical heat transport and low-velocity ablative ion blowoff with efficient momentum transfer to the target. At the somewhat higher irradiance of 7 × 10^{14} W/cm^2 the above mentioned undesirable effects are once again observed. Long, low irradiance pulses are therefore an interesting approach to laser fusion if the pellet shell can be accelerated stably. The interaction physics is reported in this letter and studies of the ablative acceleration appear elsewhere. [1,4] Also discussed herein are heat flow measurements and their relationship to laser beam uniformity requirements for successful implosion of pellets.

Manuscript submitted April 19, 1979.

The experimental arrangement is discussed in detail in Ref. 1. Planar thin foil targets of polystyrene (CH) or aluminum are mounted near the focal region of an aspheric f/10, 1-m focal length lens and are irradiated at 6° from normal incidence with a 3-nsec (FWHM) laser pulse between 10^{12} and 10^{15} W/cm^2. The target is tilted so that specular reflection can be distinguished from direct backscatter and so that the axis of symmetry of the plasma blowoff is discernable. The incident beam irradiance is adjusted, in these experiments, by varying the position of the target between the lens and its focal point. The spatial and temporal laser intensity distributions are both measured over four-decades on each shot. A uniform intensity profile is important for ablative acceleration experiments and studies of Rayleigh-Taylor instability development. Some effects caused by non-uniform illumination will be addressed below.

Absorption: Scattered light and total absorption measurements are made using a nearly 4π-sr box calorimeter[5] or an array of minicalorimeter pairs surrounding the target. The box calorimeter is used either with a pyrex shield, so that only scattered light is recorded, or without the shield, so that all emissions, scattered light, plasma, x-ray, UV, etc. are detected. The latter mode is useful as a check on the absolute calibration of the box.[1] The minicalorimeters provide similar measurements at discrete angles about the target.

The box calorimeter measures the total absorbed light to be 85 ± 10% of the incident light at 1×10^{13} W/cm^2 and 53± 10% at 7×10^{14} W/cm^2. This agrees with other determinations.[6] The 16-μm thick CH foil (apparently) goes underdense at 7×10^{14} W/cm^2 and transmission accounts for 15% of the incident energy. All the incident energy (± 10%) is accounted for when the plasma shield is removed from the box calorimeter. Figure 1 shows angular distributions of scattered light and plasma energy at three-irradiances obtained with the minicalorimeter array. (X-ray and UV emission for CH targets is < 1% of the incident energy and is therefore neglected). One notes the following general features: 1. Integration of both the scattered light

and particle energy angular distributions are in agreement with the box calorimeter results and with total energy balance. 2. The scattered light intensity peaks towards the focusing lens and at the specular angle. The backscattered portion, primarily due to Brillouin backscatter, increases rapidly with irradiance above 10^{13} W/cm^2 in agreement with measurements with laser pulses shorter than 1-nsec.[7] 3. The plasma blowoff peaks normal to the target.

Plasma Formation and Expansion: For a peak laser irradiance of 2×10^{13} W/cm,[2] plasma on the laser side of a 7-μm thick Al target is first observed (interferometrically with a $\sim$ 400 psec, 5320 Å probe pulse) 8-nsec prior to the peak of the laser pulse. This corresponds to an irradiance of $I \approx 6 \times 10^9$ W/cm^2. Initially the 10^{18} cm^{-3} density surface expands with a velocity normal to the target of 6.7×10^6 cm/sec until 2-nsec before the peak of the laser pulse ($\sim$ 20% of peak intensity), then speeds up to 3.5×10^7 cm/sec and remains constant through the peak of the pulse. This latter velocity is approximately the same as the average asymptotic ion ablation velocity measured with a time-of-flight charge collector array remote (25 cm) from the target.[1,4,9] A single ablation velocity peak is observed at $10^{12}-10^{13}$W/cm^2 whereas a second, energetic, ion component appears at 7×10^{14} W/cm^2.[1,2,8]

Electron Temperature: X-ray measurements imply information about the electron energy distribution and heat flow properties in the absorption region and target interior. Bremsstrahlung continuum measurements from 1-50 keV are obtained with an array of eleven detectors and filters located at 120° to the incident laser direction. Time-integrated x-ray spectra for CH targets are shown in Fig. 2a for irradiances of 2×10,[12] 1×10^{13} and 7×10^{14} W/cm^2. Electron temperatures of 200-400 eV for both CH and Al targets are deduced from the lower energy end of the spectra.[1] At 7×10^{14} W/cm^2, a much higher temperature (10-15 keV) is apparent in the high energy tail of the spectra. The less intense, high energy tail at 10^{13} W/cm^2 may be caused by higher irradiance hot spots on the beam. These energetic

x-ray (and hence electron) tails have been observed previously in similiar experiments[8] and are thought to be due to electron tail heating.[10] The fast ion component appearing at 7×10^{14} W/cm^2 also suggests the onset of an energetic electron component at the higher irradiance.[2]

Axial Heat Flow. An estimate of the depth of penetration of heat axially into the target is obtained by using a target consisting of a thin layer of CH overcoating an Al substrate.[3] This experiment utilizes the much higher x-ray emissivity (1-9 keV) of Al over CH. Thus, by measuring the x-ray emission characteristics of the Al substrate, i.e, spectral distributions and temporal emission, as a function of CH overlayer thickness, the depth of heat penetration is estimated. X-ray intensities, normalized to pure CH, for several CH overlayer thicknesses at 10^{13} W/cm^2, are shown in Fig. 2b. Only minimal heating of the 7-μm Al substrate is apparent for a 2-μm CH overlayer and no heating of the substrate is evident for 3.5, 4.0 and 5.0 μm overlayers. The temporal x-ray emission into the 1-2 keV range, obtained with a 0.4-nsec rise-time PIN diode with a 1-mil Be filter, is compared with the incident laser pulse in Fig. 2c. These measurements are made on separate shots using the same PIN diode and oscilloscope ($\pm$0.25 nsec jitter). A decrease in overlayer thickness from 5 μm to 2 μm causes the x-ray intensity to increase (consistent with Fig. 2b) and to be delayed relative to the laser pulse. The delayed emission indicates that the ablation layer reaches the Al substrate well after the peak of the laser pulse (but during the pulse). A similar behavior of increased, and delayed, x-ray emission is observed at an irradiance of 2×10^{12} W/cm^2 when the CH overlayer thickness is reduced from 1.2 μm to 0.6μm. Ablation depths inferred using the layered target technique are consistent with mass accounting inferred from calorimetry and time-of-flight measurements.[4]

Lateral Heat Flow. Lateral heat flow acts as a heat loss mechanism from the interaction region. On the other hand, sufficient lateral heat conductivity can prevent hot spots on the

incident beam from producing uneven target acceleration and triggering hydrodynamic instabilities.

A suggestion that the lateral heat flow is not sufficient to eliminate the effects of laser intensity variations, at least in the region of 1-keV x-ray emission (a few times n_c) [11,12] is seen in Fig. 3. Here laser focal distributions are compared with iso-density contours from x-ray pinhole photographs of the rear of (optically thin) CH foil targets. Intensity lobes are deliberately introduced into the focal distribution by placing varying widths of an opaque strip across the center of the focusing lens (a crude coded aperture). Note that the hot spot details of the x-ray image correlate well with those in the incident beam.[13] The effect of 3:1 variations in the beam focal spot distribution results in approximately a 2:1 variation in the x-ray intensity (which implies a temperature differential of $\approx$ 25% i.e., 75 eV). This temperature differential is consistent with the value calculated from classical heat conductivity given the size of the laser beam nonuniformities and the plasma temperature interred from x-ray measurements. Thus it appears that under our experimental conditions, (classical) heat flow is not sufficient to wash out lateral temperature gradients near the critical density due to gross (3:1) beam nonuniformities involving scale lengths greater than 30 μm.

However, the more important question is whether these non-uniformities are transmitted to the ablation surface and thus to the accelerating target. This is demonstrated to be true, for gross non-uniformities, by comparing protrusions on the rear of the foil in Fig. 3 (observed by optical interferometry) to the intensity lobes introduced onto the incident beam profile. Clearly the laser beam uniformity here is not sufficient for pellet compression. Other indications that lateral heat flow is low for our conditions are that the width of the ablatively accelerated portion of the target, observed interferometrically and via a Doppler shift technique, remains approximately the size of the focal diameter.[1,4]

We have shown here that for long low-irradiance 1.06-μm laser pulses ($3 \times 10^{12} - 1 \times 10^{13}$ W/cm^2, 3-nsec) the absorption process is very efficient (>80%) with minimal Brillouin backscatter and non-thermal electron heating. Low electron temperatures and good axial heat transport yield ion ablation velocities well suited for efficient acceleration of laser fusion pellet shells. This low-irradiance regime has therefore many characteristics favorable to laser fusion. Hot regions in the x-ray emission, due to corresponding non-uniformities in the focal spot distribution, suggest that lateral heat flow is low but near classical. As a consequence, gross beam non-uniformities are transmitted to the ablation surface.

The contributions of the following in this work is appreciated: S. E. Bodner, J. A. Stamper, J. Grun, P. Moffa, S. Gitomer, J. Boris, S. H. Gold, M. Fink, N. Nocerino, E. Turbyfill, C. M. Dozier and J. W. Criss. This work is supported by the U.S. Dept. of Energy.

REFERENCES

a) Present association: Sachs-Freeman Assoc., Bladensburg, Md.

1. NRL Laser-Plasma Interaction Group, NRL Memo. No. 3890 (1978) ed. B.H. Ripin

2. B.H. Ripin, et al., Phys. Rev. Lett. **39**, 611 (1977); R. Decoste and B.H. Ripin, Phys. Rev. Lett. **40**, 34 (1978); D.W. Phillion, W.L. Kruer and V.C. Rupert, Phys. Rev. Lett. **39**, 1529 (1977); E.K. Storm, et al., Phys. Rev. Lett. **40**, 1570 (1978).

3. F.C. Young, et al, Appl. Phys. Lett. **30**, 45 (1977); B. Yaakobi and T.C. Bristow, Phys. Rev . Lett. **38**, 350 (1977); and A. Zigler et al., J. Phys. D: Appl. Phys. **10**, L159 (1977).

4. R. Decoste, et al., to be published.

5. S.R. Gunn, Lawrence Livermore Lab. UCID-17308 (1976); and R.R. Whitlock, to be published.

6. J. P. Anthes, et al., Bull. Am Phys. Soc. **23**, 777 (1978).

7. B.H. Ripin, et al., Phys. Rev. Lett. **33**, 634 (1974).

8. N.G. Basov, et al, Sov. J. Quantum Electron. **3**, 444 (1974), [Kvantovaya Elektron **5**, 126 (1973)]; R.A. Haas, et al, Phys, Rev. Lett. **39**, 1533 (1977); and J. S. Pearlman and J. P. Anthes, Appl. Phys. Lett. **27**, 581 (1975).

9. J.P. Anthes, M.A. Gusinow and M.K. Matzen, Phys. Rev. Lett, **41**, 1300 (1978); M.A. Gusinow, et al., Appl. Phys. Lett. **33**, 800 (1978); and M.K. Matzen and R.L. Morse, Bull. Am. Phys. Soc. **23**, 787 (1978).

10. C.M. Armstrong, et al, NRL Memo No. 3829 (1978) (to be published).

11. B.H. Ripin, et al, Phys Rev. Lett. **34**, 1313 (1975).

12. P.J. Moffa, J.H. Orens and J.P. Boris, to be published.

13. Similar hot spots were observed above 10^{14} W/cm^2 in x-ray pinhole photos taken of the front side of a target in: H.D. Shay, et al, Phys. Fluids **21**, 1634 (1978).

14. L. Spitzer, "Physics of Fully Ionized Gases," (J. Wiley, New York 1961.)

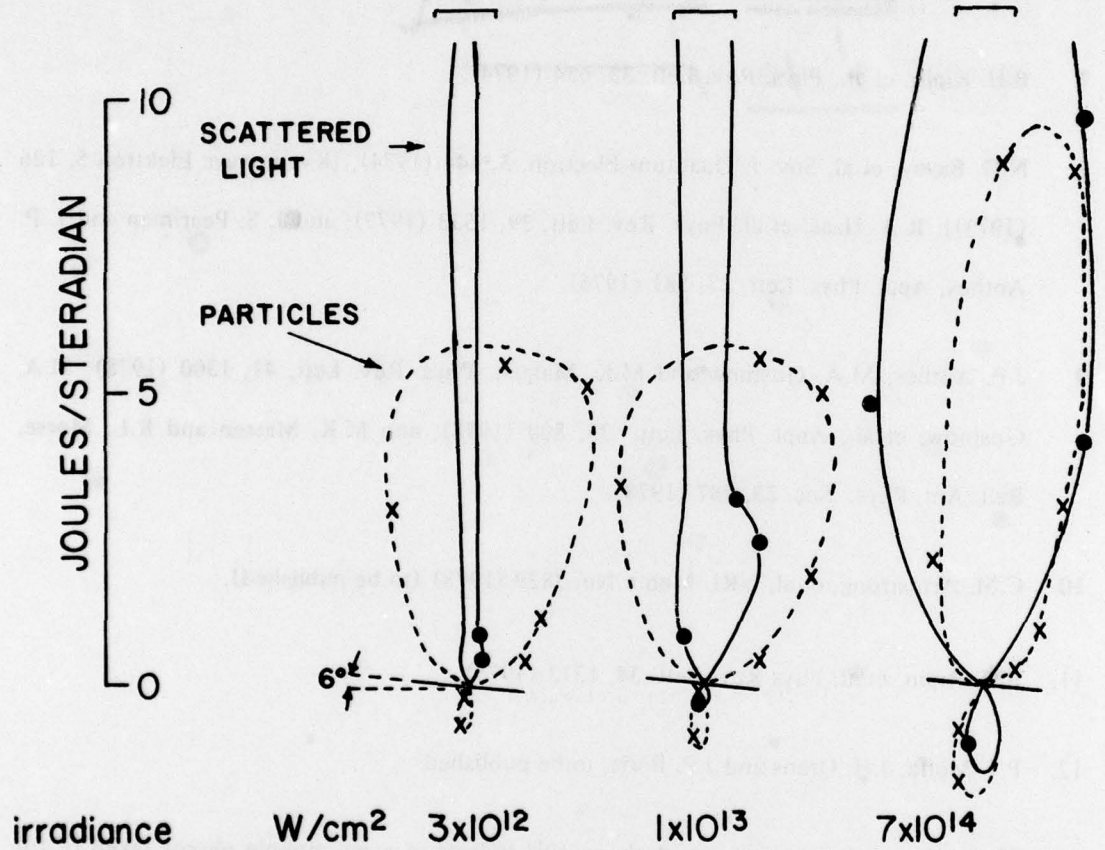

Fig. 1 — Angular distributions of scattered light and plasma blowoff energy at three irradiances. Incident energies, focal spot diameters and CH target thickness were respectively: (10.7J, 450 μm, 10 μm), (15.3J, 230 μm, 16 μm) and (16.1J, 35 μm, 16 μm). Laser light is incident vertically from the top through the solid angles represented by bars.

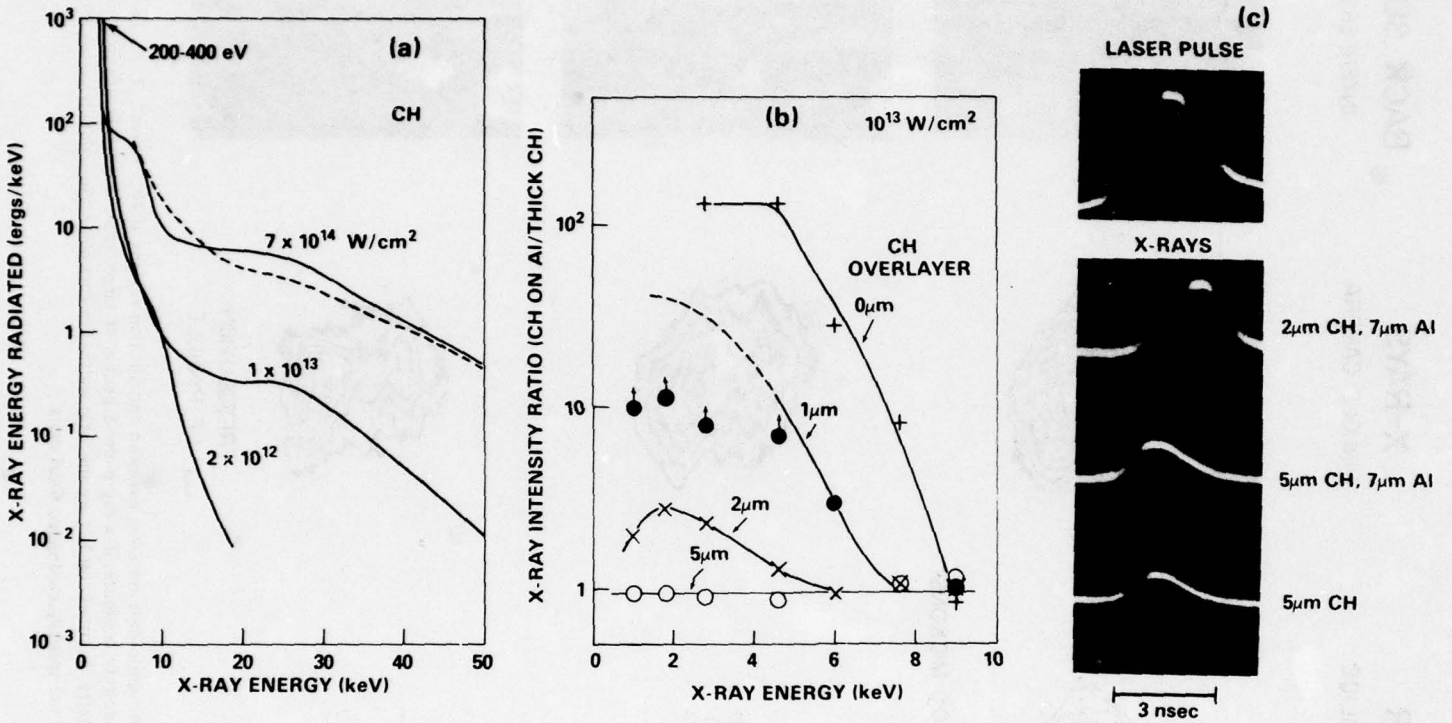

Fig. 2(a) — X-ray spectra measured with CH foil targets irradiated at 2×10^{12}, 1×10^{13} and 7×10^{14} W/cm^2. Dashed spectrum is for 5×10^{15} W/cm^2, 5J, 75-psec pulse. (b)— X-ray intensity ratios for layered targets at x-ray energies from 1 to 9 keV. The data below 5 keV for a 1-μm thick CH overlayer correspond to lower limits due to saturation of the detector amplifiers. (c)—A temporal comparison of the emission of 1-2 keV x-rays and the incident laser pulse ($\sim 10^{13}$ W/cm^2) for different layered targets. Amplitude scales are the same for all three x-ray traces.

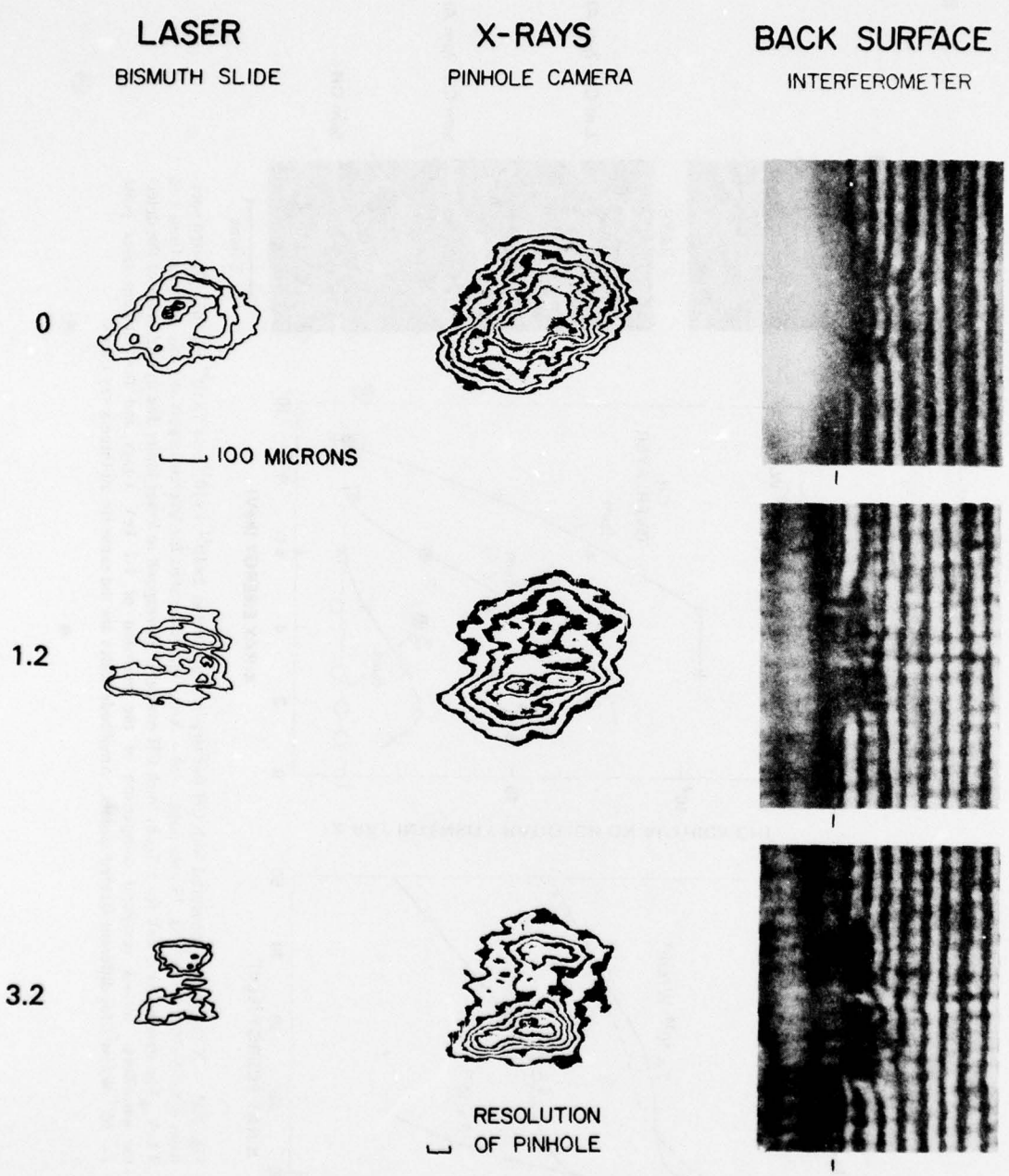

Fig. 3 — Effect of beam non-uniformity on x-ray emission and ablation regions at 10^{13} W/cm^2. Left: Laser focal spot distributions. Middle: Isodensity contours of x-ray pinhole photos of target rear. Right: Protrusions on target rear surface seen via interferometry. Numbers on left are the strip widths (in cm) placed horizontally across the lens diameter (8 cm) used to produce the spatially modulated focal spots.